Dynamics of Ultra-precision Machining and Its Effect on Surface Roughness

Changqing Cheng Satish T.S. Bukkapatnam
Department of Industrial & Systems Engineering
Texas A & M University

Outline

- **Introduction**
  - Why ultra-precision machining (UPM)
- **Background and literature review**
  - Research challenge and gap
- **Methodology**
  - **Physics-based model:** process dynamics analysis using delayed differential equation
  - **Statistical model:** sensor-based surface roughness estimation
- **Results**
- **Summary and future work**

Introduction

- Development of **sensor-based technique:** especially in advanced manufacturing processes control
  - Aerospace, biomedical, electronics, automotive *et al.* (Lee 1999, Liu 2004)
- **Taniguchi curve:** nano-metric manufacturing accuracy
  - Industry relies on **ultra-precision machining (UPM)** to realize **surface roughness (Ra)** at 10 nm – 30 um

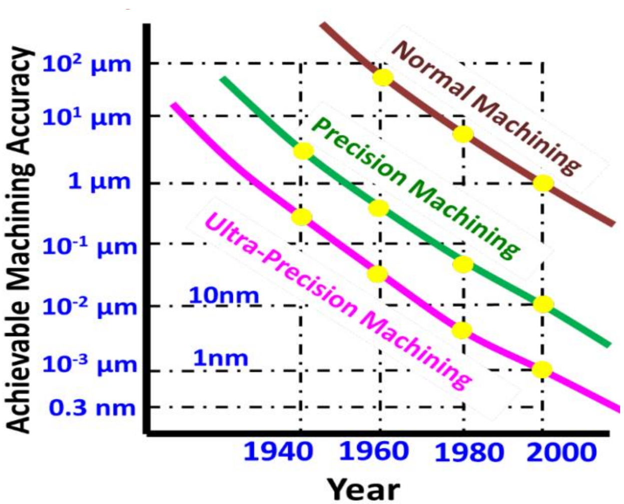

Taniguchi 1983

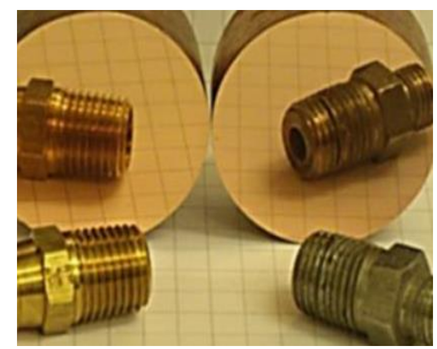

Challenge in UPM

- **Quality issue:** anomaly development (even in well-designed process) cannot be predicted

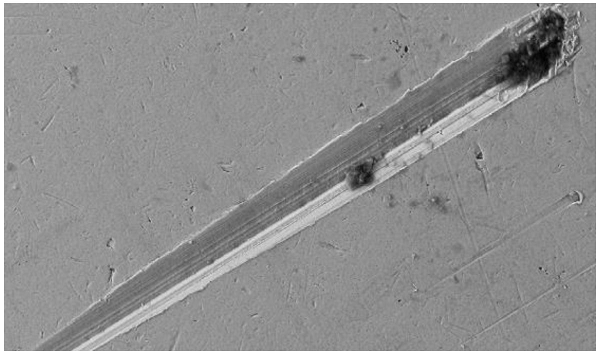

High-definition optical inspection

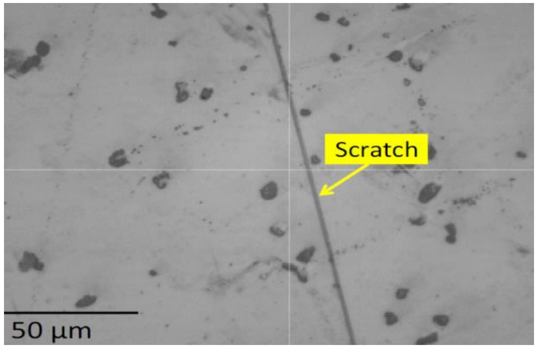

Prahalad 2013

- **Physics-based models:** cannot predict surface change
  - **Cutting mechanics:** cutting stresses (Marsh 2005); micro-plasticity effect (Yuan 1994, Lee 2001); tool interference (Cheung 2003); material recovery and swelling effect (Kong 2006)
  - **Micro-physics:** crystallographic orientation of the grain (Lee 2000); metrology and process physics (Dornfeld et al. 2006)
  - **Spectrum analysis:** Ra spectrum component (Cheung and Lee 2000, Pandit and Shaw 1981, Hocheng et al. 2004)

Surface roughness models

- **Sensor-based analytics models:** applicable for real-time Ra estimation
  - **Vibration analysis:** vibration amplitude and frequency (Lin 1998, Abouelatta and Madl 2001, Liu 2004)
  - **Acoustic emission** (Beggan et al. 1999)
  - **Temperature sensor** (Hayashi et al. 2008)
  - **Strain gauge sensor** (Shinno et al. 1997)
- Limited by *nonlinear* and *nonstationary* nature of machining signals

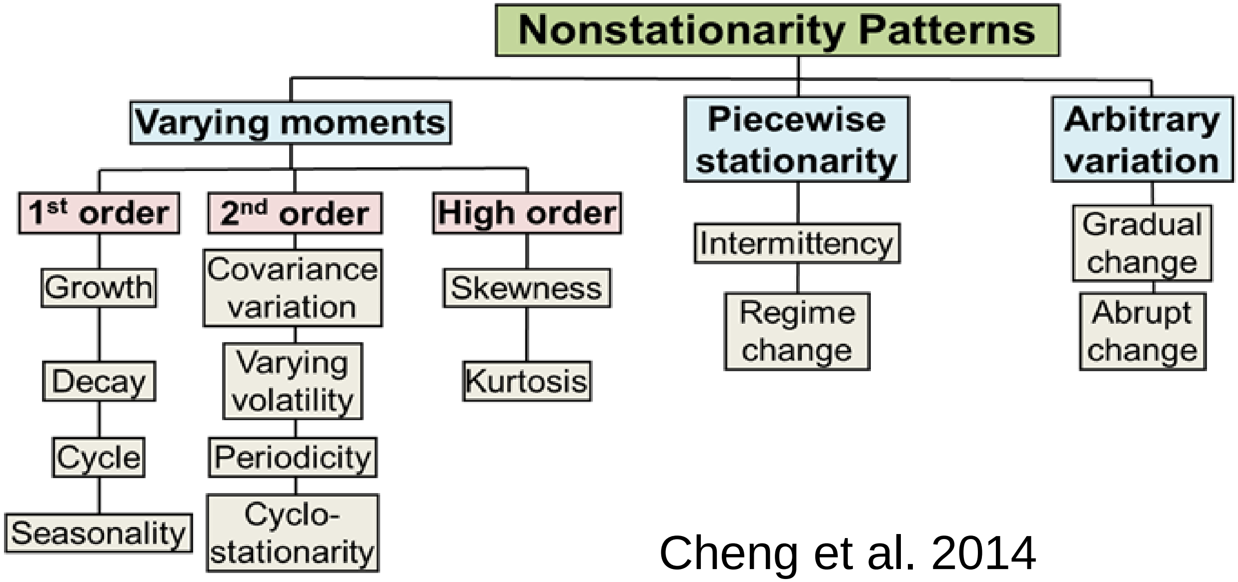

Cheng et al. 2014

Approach

- **Physics domain model:** consider tool radius effect, ploughing and shearing effect, elastic material recovery; predict system dynamic response
- **Sensor-based model:** extract information from *in situ* signals; detect change in the process

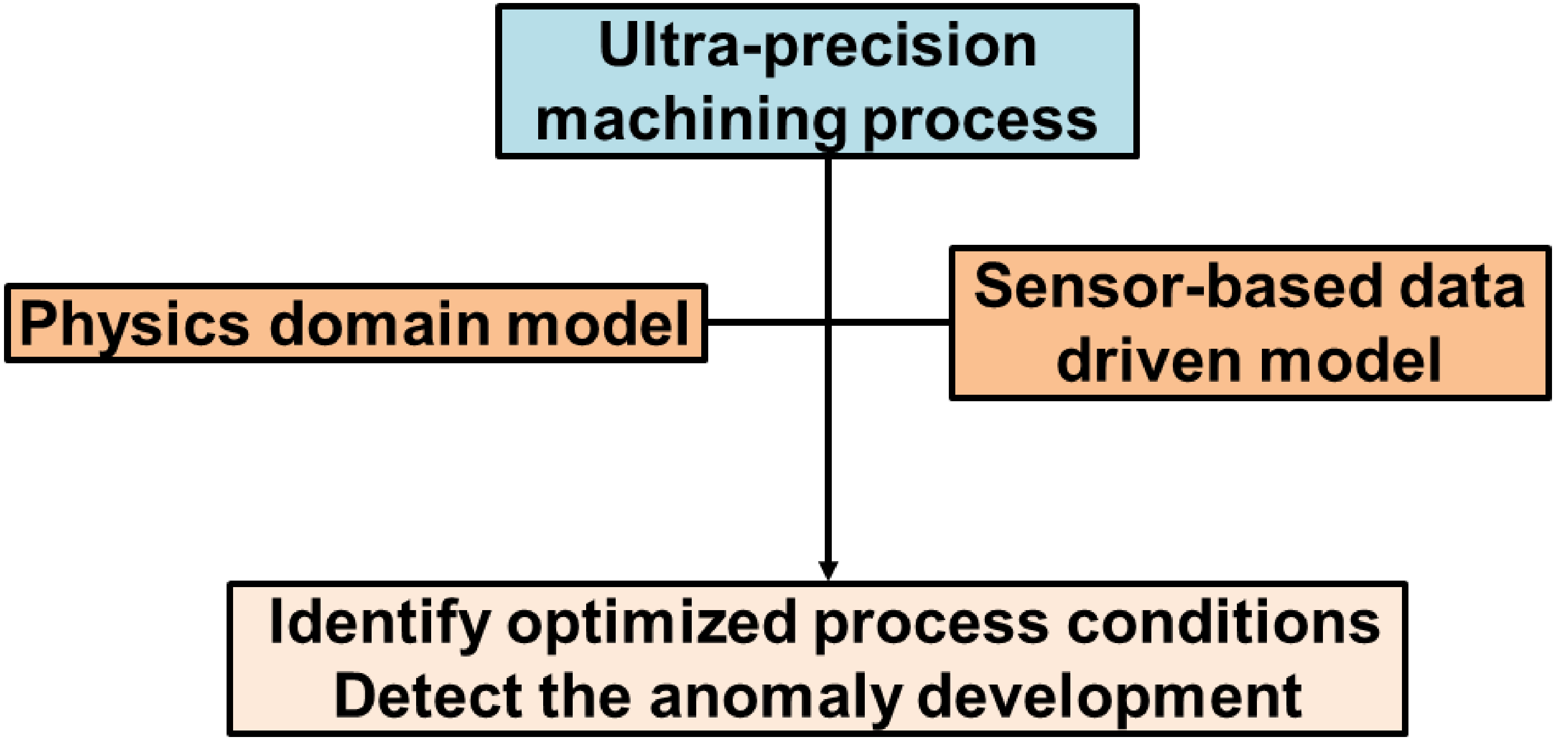

Process dynamics

- **3 types of vibrations:** free vibration, forced vibration, and **self-excited vibration (chatter)** (Tobias 1961)
  - **Frictional chatter:** ploughing on the work-piece surface
  - **Regenerative chatter:** overlapping cuts; source for vibration amplification
  - Bring system to instability
  - Result in inferior part surface and increase tool wear
  - Most undesirable and least controllable (Quintana et al 2011)
- How to model the chatter at **UPM** is still not well addressed.

Quintana et al 2011

UPM dynamics model

$$\ddot{y}(t) + 2\zeta\omega_n\dot{y}(t) + \omega_n^2 y(t) = -\frac{F\big(y(t),y(t-T)\big)}{m}$$

y: tool displacement

T: period length, $T = \frac{1}{\Omega}$

Process parameters: feed f_0, spindle speed Ω, chip width w

Thrust force model: shearing and ploughing components

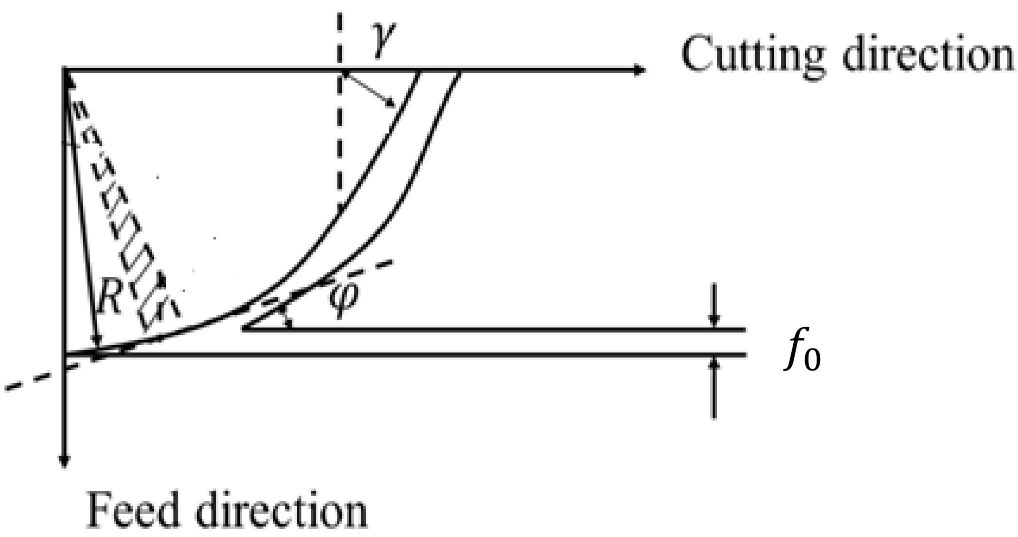

$f_0 \geq f_{min}$: material removal; both shearing and ploughing forces exist

$f_0 < f_{min}$: only elastic deformation and ploughing force

Shearing Force

- **Dynamic chip thickness**

$$t_u = (f_0 - y(t) + y(t - T)) - \delta$$

- **Shearing angle** (Waldorf et al 1999)

$$\phi = \tan^{-1} \frac{f_0 - \delta}{R\tan\left(\frac{\pi}{4} + \frac{\alpha}{2}\right) + \frac{\delta}{\tan(\frac{\pi}{2} + \alpha)} - \sqrt{2R\delta - \delta^2} + t_c / \cos\alpha - f_0 \tan\alpha}$$

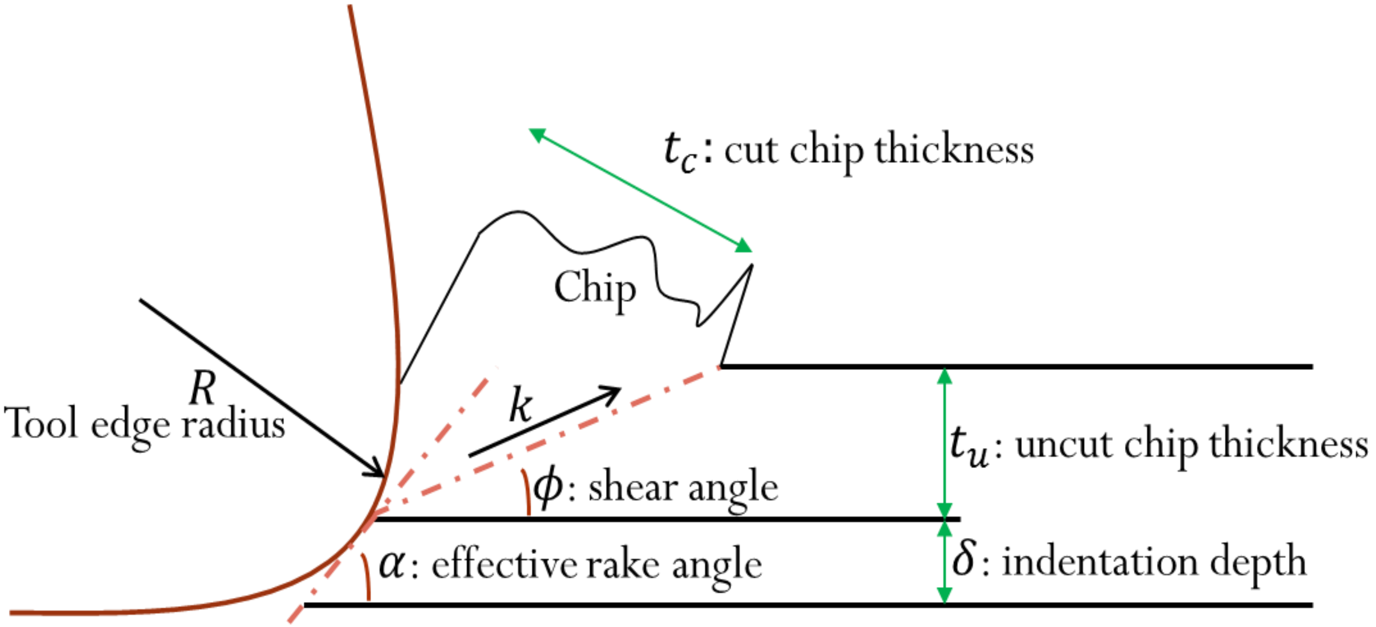

Thrust Force

- **Shearing component**
  - **Shearing** force parallel to shearing plane

$$F_s = kt_u w / \sin\phi \qquad (w\text{: chip width/ depth of cut})$$

  - **Normal** force on shearing plane

$$F_n = F_s[1 + 2(\frac{\pi}{4} - \phi)]$$

  - Contribution to **thrust** force

$$F_t(1) = F_n \cos\phi \; - F_s \sin\phi = kw\left[\left(1 + \frac{\pi}{2} - 2\phi\right)\cot\phi - 1\right]t_u$$

- **Ploughing component** (Waldorf 1999)
  - **Elastic model:** cylinder indentation on an elastic surface
  - Contribution to **thrust** force

$$F_t(2) = \frac{2.375\pi w E}{8(1-\nu^2)}\delta$$

$$\frac{F_t(1)}{m} = Akwt_u \qquad \frac{F_t(2)}{m} = B\delta$$

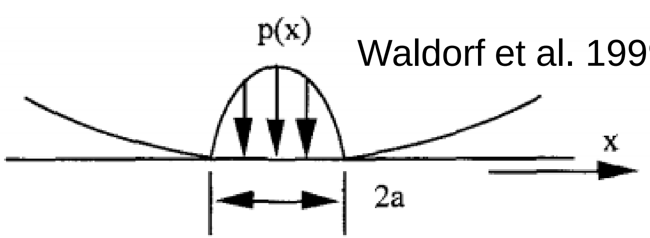

Waldorf et al. 1999

Process dynamics

- **Delayed differential equation** for tool dynamics

$$\ddot{y}(t) + 2\zeta\omega_n\dot{y}(t) + \omega_n^2 y(t) = -\frac{F_t(1) + F_t(2)}{m} = -At_u - B\delta$$
$$= -Akwf_0 - Akw[y(t) - y(t-T)] + \delta(Akw - B)$$
$$= -Akw[y(t) - y(t-T)] + C$$

- No closed-form solution to **dynamics state**: $y(t)$
- **Temporal finite element model** can be used for approximation (Bayly et al. 2003, Khasawneh et al. 2009)
  - The time per revolution $\boldsymbol{T}$ is divided into $\boldsymbol{M}$ elements
  - Approximation to the solution for the tool displacement on each element

$$y_j^n(\tau) = \sum_{i=1}^{4} a_{ji}^n S_i(\tau) \qquad y_j^{n-1}(\tau) = \sum_{i=1}^{4} a_{ji}^{n-1} S_i(\tau)$$

τ: local time, $0 \le \tau \le t_j$; t_j: time for element j, $t_j = \frac{T}{M}$

Temporal finite element model (TFEM)

- Hermite basis functions (Mann et al. 2006)

$$S_1(\tau) = 1 - 3\left(\frac{\tau}{t_j}\right)^2 + 2\left(\frac{\tau}{t_j}\right)^3$$

$$S_2(\tau) = t_j\left[\frac{\tau}{t_j} - 2\left(\frac{\tau}{t_j}\right)^2 + \left(\frac{\tau}{t_j}\right)^3\right]$$

$$S_3(\tau) = 3\left(\frac{\tau}{t_j}\right)^2 - 2\left(\frac{\tau}{t_j}\right)^3$$

$$S_4(\tau) = t_j\left[-\left(\frac{\tau}{t_j}\right)^2 + \left(\frac{\tau}{t_j}\right)^3\right]$$

- Orthogonal; second-order continuous
- Coefficients represent the **state variable** (displacement and velocity) at the beginning/end of each element
- Boundary conditions

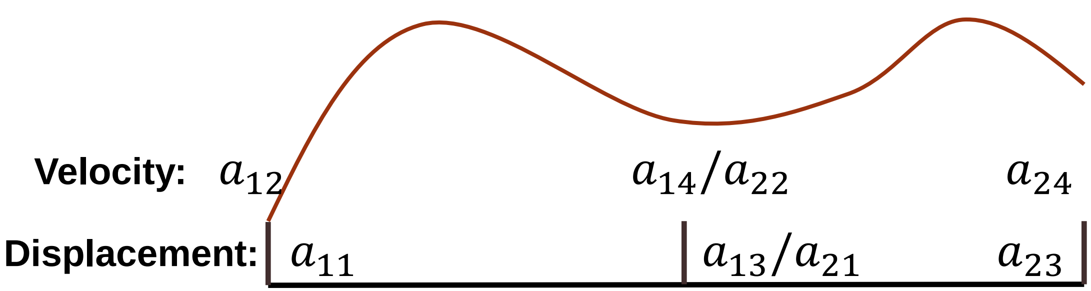

TFEM

- Approximation leads to non-zero **error**

$$\sum_{i=1}^{4} a_{ji}^{n}\ddot{\phi}_i + 2\zeta\omega_n \sum_{i=1}^{4} a_{ji}^{n}\dot{\phi}_i + \omega_n^2 \sum_{i=1}^{4} a_{ji}^{n}\phi_i + Akw\left[\sum_{i=1}^{4} a_{ji}^{n}\phi_i - \sum_{i=1}^{4} a_{ji}^{n-1}\phi_i\right] - C = error$$

- **Method of weighted residuals** (Reddy 1993)

Independent trial functions: $\psi_1 = 1 \qquad \psi_2 = \frac{2\tau}{t_j} - 1$

$$\int_0^{t_j}\left[\sum_{i=1}^{4} a_{ji}^{n}\ddot{\phi}_i + 2\zeta\omega_n \sum_{i=1}^{4} a_{ji}^{n}\dot{\phi}_i + \omega_n^2 \sum_{i=1}^{4} a_{ji}^{n}\phi_i + Akw\left(\sum_{i=1}^{4} a_{ji}^{n}\phi_i - \sum_{i=1}^{4} a_{ji}^{n-1}\phi_i\right) - C\right]\psi_p(\tau)d\tau = 0$$

TFEM

$$\sum_{i=1}^{4} a_{ji}^{n} \int_{0}^{t_j} [\ddot{\phi}_i + 2\zeta\omega_n\dot{\phi}_i + (\omega_n^2 + Akw)\phi_i]\, \psi_p(\tau)d\tau = \sum_{i=1}^{4} a_{ji}^{n-1} \int_{0}^{t_j} Akw\phi_i\, \psi_p(\tau)d\tau + \int_{0}^{t_j} C\psi_p(\tau)d\tau$$

$\Rightarrow$

$$\sum_{i=1}^{4} a_{ji}^{n} N_{pi}^{j} = \sum_{i=1}^{4} a_{ji}^{n-1} P_{pi}^{j} + Q_p^j$$

$$N_{pi}^{j} = \int_{0}^{t_j} [\ddot{\phi}_i + 2\zeta\omega_n\dot{\phi}_i + (\omega_n^2 + Akw)\phi_i]$$

$$P_{pi}^{j} = \int_{0}^{t_j} Akw\phi_i\, \psi_p(\tau)d\tau$$

$$Q_p^j = \int_0^{t_j} C\psi_p(\tau)d\tau$$

- $M = 2$; **boundary continuous conditions**
- Matrix format

$$\begin{bmatrix} 1 & 0 & 0 & 0 & 0 & 0 \\ 0 & 1 & 0 & 0 & 0 & 0 \\ N_{11} & N_{12} & N_{13} & N_{14} & 0 & 0 \\ N_{21} & N_{22} & N_{23} & N_{24} & 0 & 0 \\ 0 & 0 & N_{11} & N_{12} & N_{13} & N_{14} \\ 0 & 0 & N_{21} & N_{22} & N_{23} & N_{24} \end{bmatrix} \begin{bmatrix} a_{11} \\ a_{12} \\ a_{21} \\ a_{22} \\ a_{23} \\ a_{24} \end{bmatrix}^{n}$$

$$= \begin{bmatrix} 0 & 0 & 0 & 0 & 1 & 0 \\ 0 & 0 & 0 & 0 & 0 & 1 \\ P_{11} & P_{12} & P_{13} & P_{14} & 0 & 0 \\ P_{21} & P_{22} & P_{23} & P_{24} & 0 & 0 \\ 0 & 0 & P_{11} & P_{12} & P_{13} & P_{14} \\ 0 & 0 & P_{21} & P_{22} & P_{23} & P_{24} \end{bmatrix} \begin{bmatrix} a_{11} \\ a_{12} \\ a_{21} \\ a_{22} \\ a_{23} \\ a_{24} \end{bmatrix}^{n-1} + \begin{bmatrix} 0 \\ 0 \\ Q_1 \\ Q_2 \\ Q_1 \\ Q_2 \end{bmatrix}$$

$$\boldsymbol{N}\boldsymbol{a}^{n} = \boldsymbol{P}\boldsymbol{a}^{n-1} + \boldsymbol{Q}$$

Stability analysis

- $\boldsymbol{a}^{n} = \boldsymbol{G}\boldsymbol{a}^{n-1} + \boldsymbol{N}^{-1}\boldsymbol{Q}$ ($\boldsymbol{G} = \boldsymbol{N}^{-1}\boldsymbol{P}$ Monodromy operator)
- **Criterion:** asymptotic stability requires eigenvalues of $\boldsymbol{G}$ within the unit circle of the complex plane
  - Maximum absolute eigenvalues $< \mathbf{1}$
- **Stability lobe diagram**
  - Map the area of **stability** as a function of the **machining parameters** (feed, depth of cut, and spindle speed)
  - Identify the **optimum conditions** that **maximize** the chatter-free **material removal rate** and avoid **inferior surface**

Sensitivity analysis

- **Stability sensitivity** on δ with perturbation $d\delta$

$$\tan\phi' = \tan\phi + \left[-R\tan\left(\frac{\pi}{4}+\frac{\alpha}{2}\right) - \frac{t_c}{\cos\alpha} + f_0\cot\alpha\right] + \frac{f_0 R + (R-f_0)\delta}{\sqrt{2R\delta-\delta^2}}\,d\delta$$

$C_0 \ll \tan\phi$, $C_0 = 0$

$$A' \approx \left[\frac{1+\frac{\pi}{2}}{\tan\phi} + \frac{2(\tan\phi)^2}{3} - 3\right] + \left[\frac{2\tan\phi\,(f_0R+(R-f_0)\delta)}{3\sqrt{2R\delta-\delta^2}} - \frac{(1+\frac{\pi}{2})(f_0R+(R-f_0)\delta)}{\sqrt{2R\delta-\delta^2}(\tan\phi)^2}\right]d\delta$$

Sensitivity analysis

- **2-element** maximum eigenvalue analysis

$$\lambda'_{max} \approx \lambda_{max} + \frac{(\tan\phi')^2}{\tan\phi + \frac{f_0 R + (R - f_0)\delta}{\sqrt{2R\delta - \delta^2}} d\delta} \left(\frac{1 + 2\left(\frac{\pi}{4} - \phi'\right)}{tan\phi\prime} - 1 \right) \left(1 + \frac{\pi}{2}\right) + \frac{\tan\phi\sqrt{2R\delta - \delta^2}}{\left(1 + \frac{\pi}{2}\right)\sqrt{f_0 R + (R - f_0)\delta}} d\delta$$

- Given $d\delta = \pm 0.2\delta$, $\lambda'_{max} \approx \lambda_{max} \pm 0.08$

- **Uncertainty** for stability boundary: $|\lambda_{max}|$ close to 1

UPM experiment setup

- **Face turning** of aluminum alloy disk-shaped workpiece
- **Cutting tools:** polycrystalline diamond ($R = 60\ um$)
- **Vibration sensors:** Kistler 8782A500
- **Force sensors:** 3-axis piezoelectric dynamometer Kistler A9251A

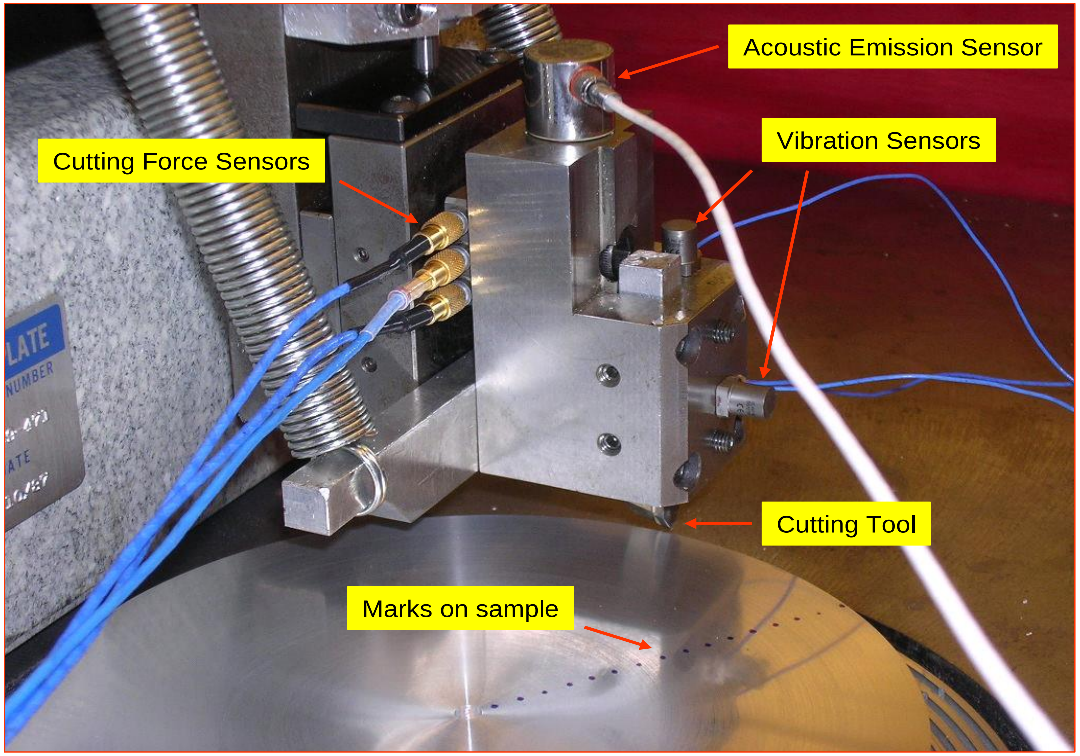

Feed = 12 / 6 um per revolution

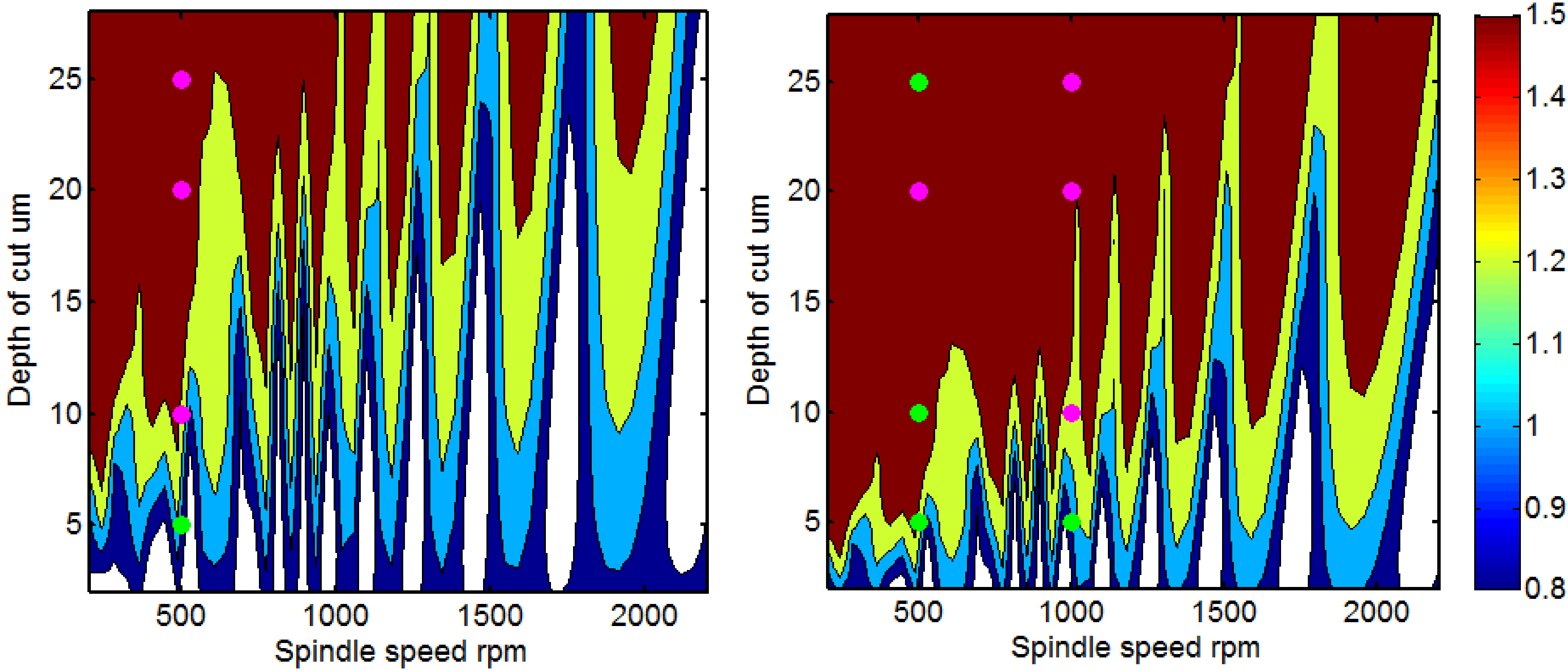

- Ra measured from MicroXAM® for chatter identification
- $Ra > 100\ nm$: onset of the chatter

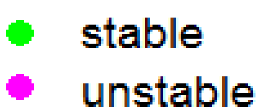

Feed = 3 / 1.5 um per revolution

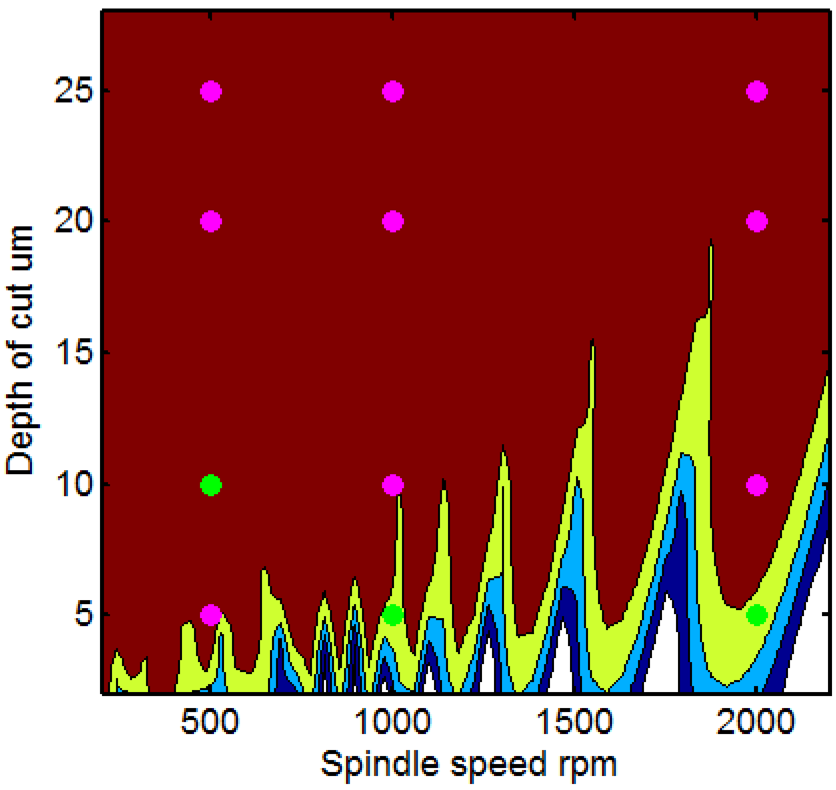

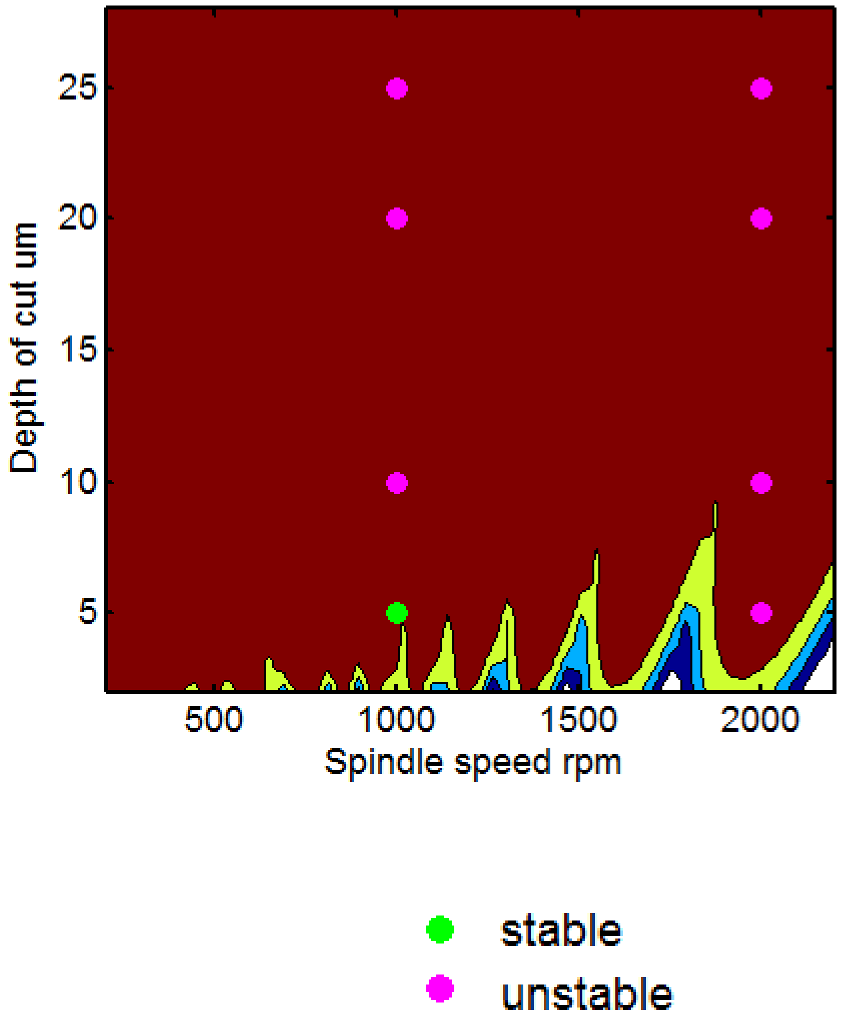

Feed = 0.75 um per revolution

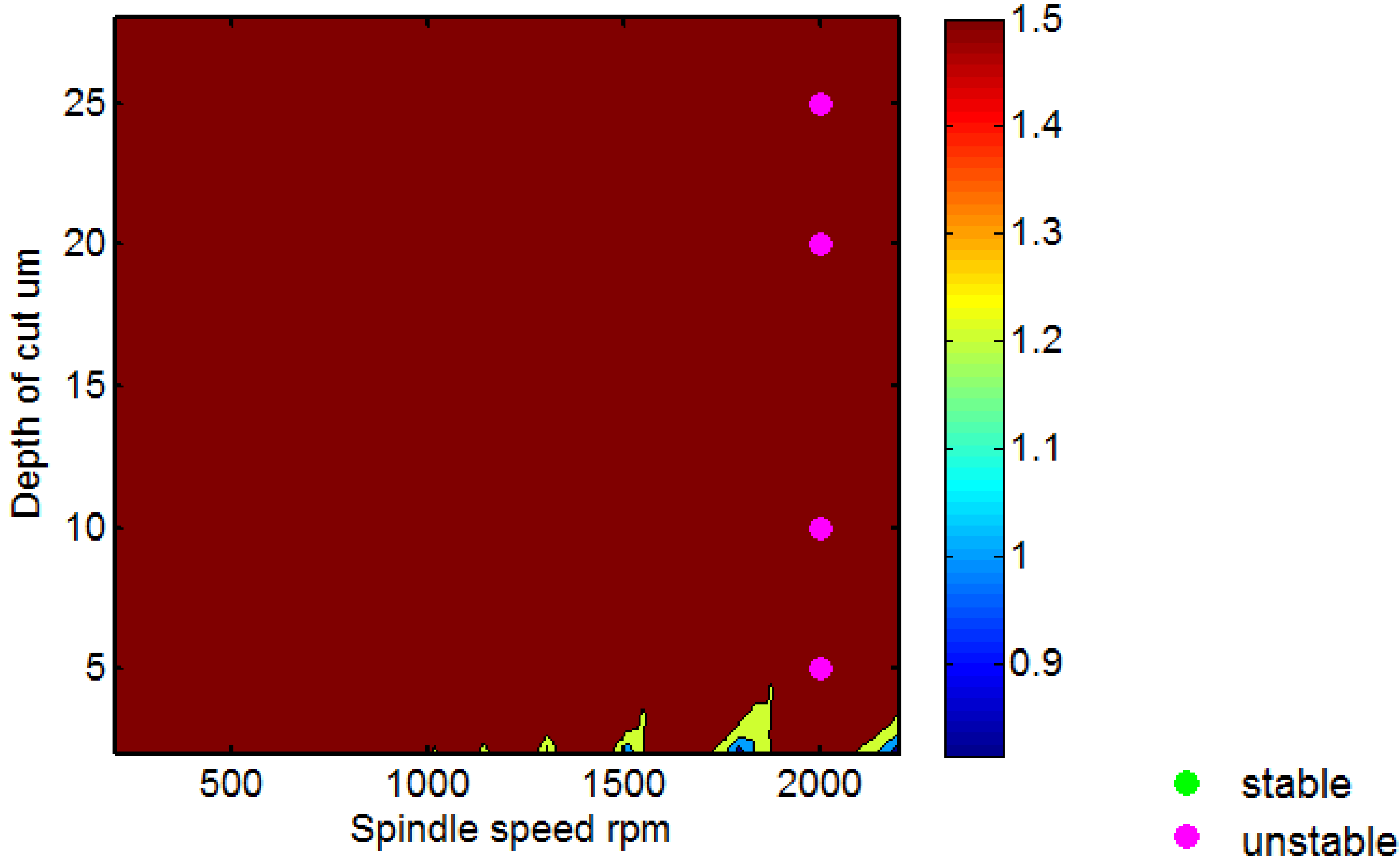

- $f_0 < 0.75\ um/\text{revolution}$: no material removal/chip formation; only ploughing; high surface roughness

Summary for physics-based model

- **Delayed differential equation (DDE)** with **temporal finite element model (TFEM)**
  - Investigate the process dynamics for UPM
  - Consider the dynamic **shearing and ploughing** forces at nano-scale machining
  - Can identify **optimum conditions**, tending to generate low surface roughness
- **Challenges**
  - Surface roughness Ra varies according to **chip formation process** and other **uncontrollable factors** even under optimum conditions
  - Ra variation monitoring in the incipient stages in real-time given process parameters; vital for nano-metric range finish assurance

Physics-based sensor fusion technique for Ra real-time estimation

Sensor-based model

- **Feature extraction**
  - Difficult to evaluate UPM process from the **raw time series** signals
  - Transform time series into **feature space** with *reliable*, *effective* and *accurate* features
  - Identify the **patterns** hidden into the raw signals

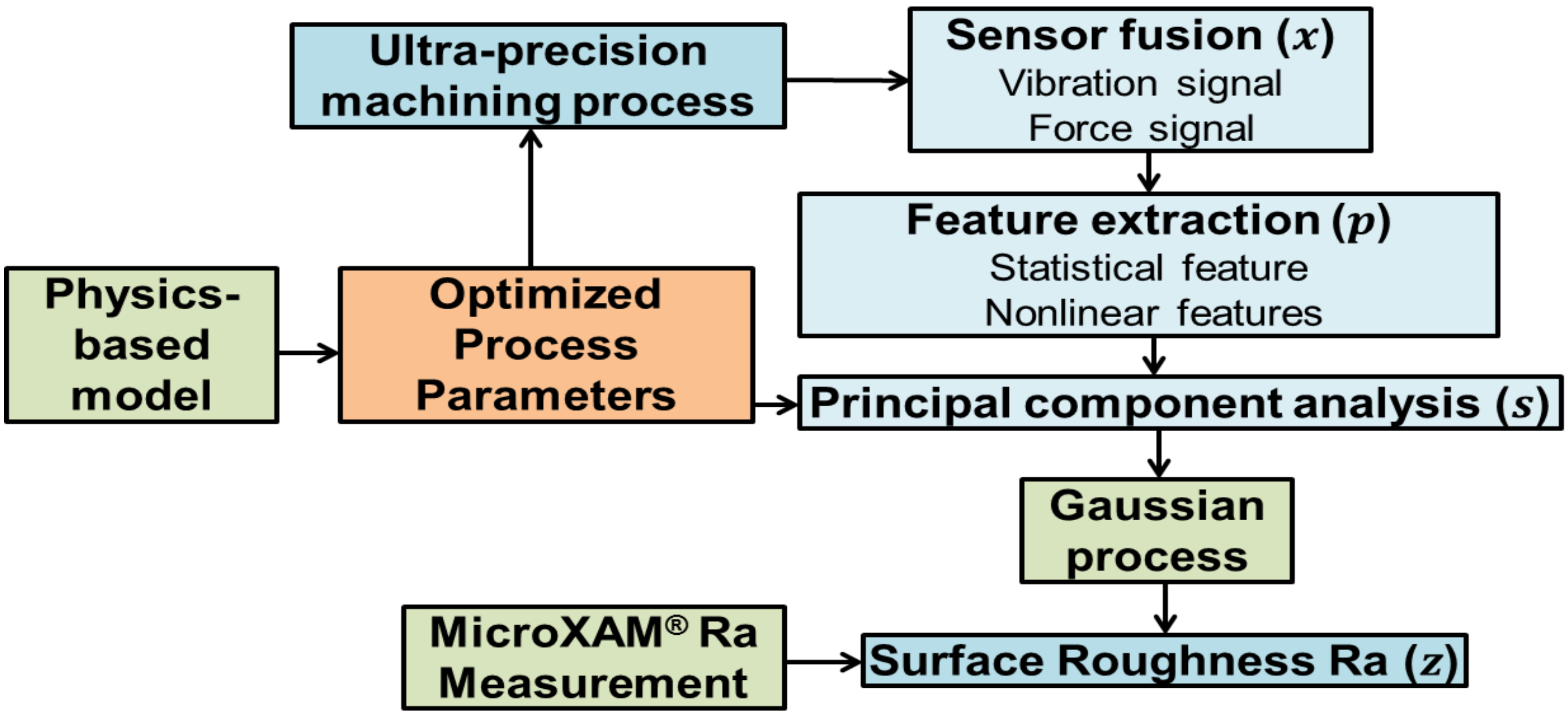

Statistical features

Absolute mean	$p_1 = \frac{1}{N}\sum_{i=1}^{N} \lvert x_i \rvert$
Standard deviation	$p_2 = \sqrt{\frac{1}{N}\sum_{i=1}^{N}(x_i - u)^2}$
Skewness	$p_3 = \frac{\sum_{i=1}^{N}(x_i - u)^3}{N p_2^3}$
Kurtosis	$p_4 = \frac{\sum_{i=1}^{N}(x_i - u)^4}{N p_2^4}$
Root mean square	$p_5 = \sqrt{\frac{1}{N}\sum_{i=1}^{N} x_i^2}$

Recurrence quantification analysis

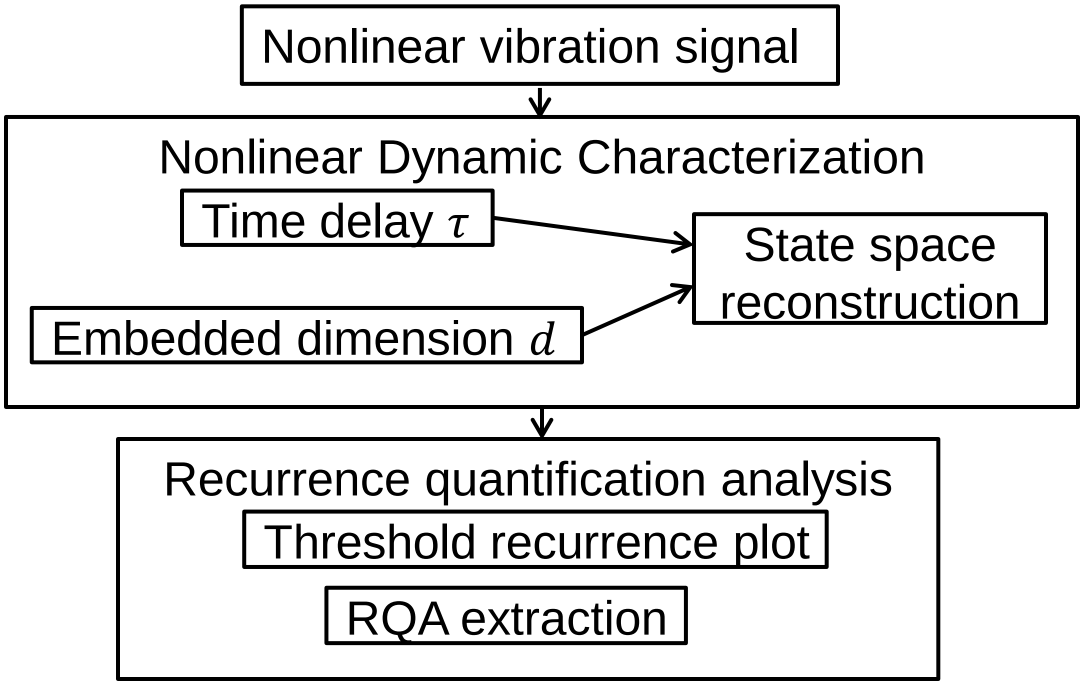

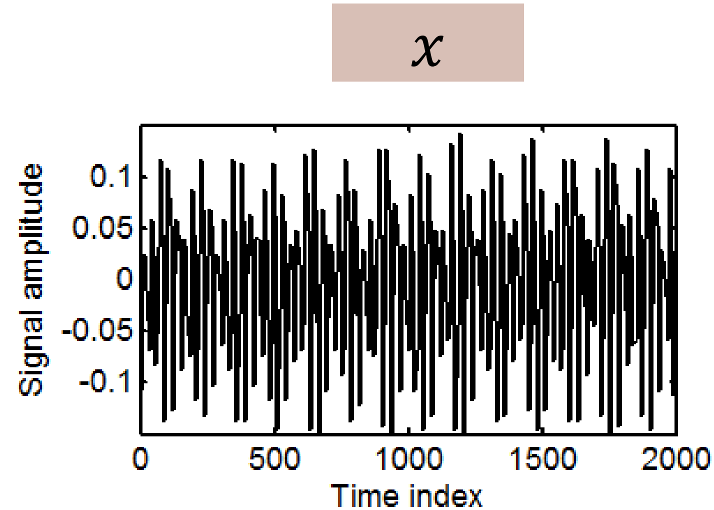

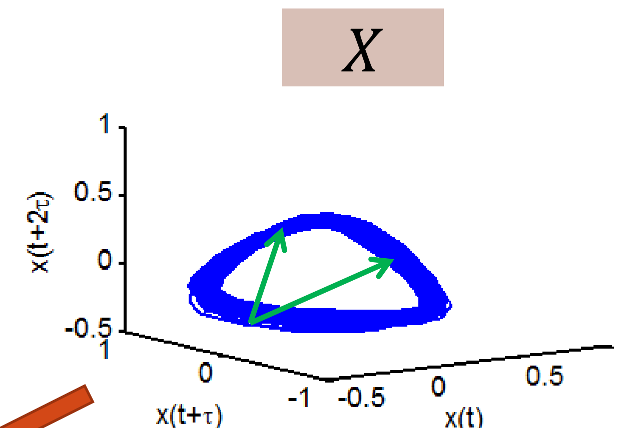

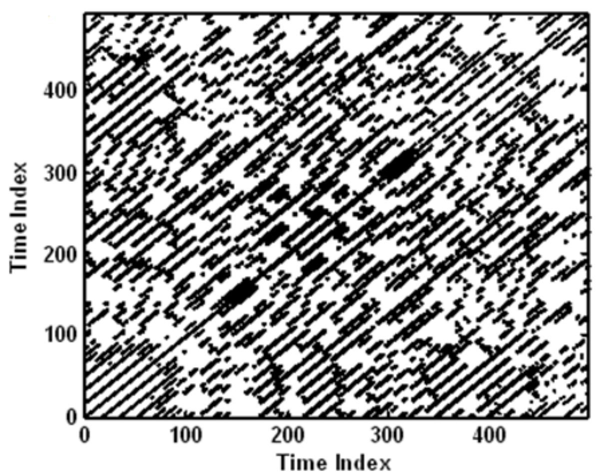

PCA

- Total number of variables: $3 + 6 \times 9 = 57$
- The first 3 principal components explained over 70% of the total variance
- Contribution to the 1st principal component

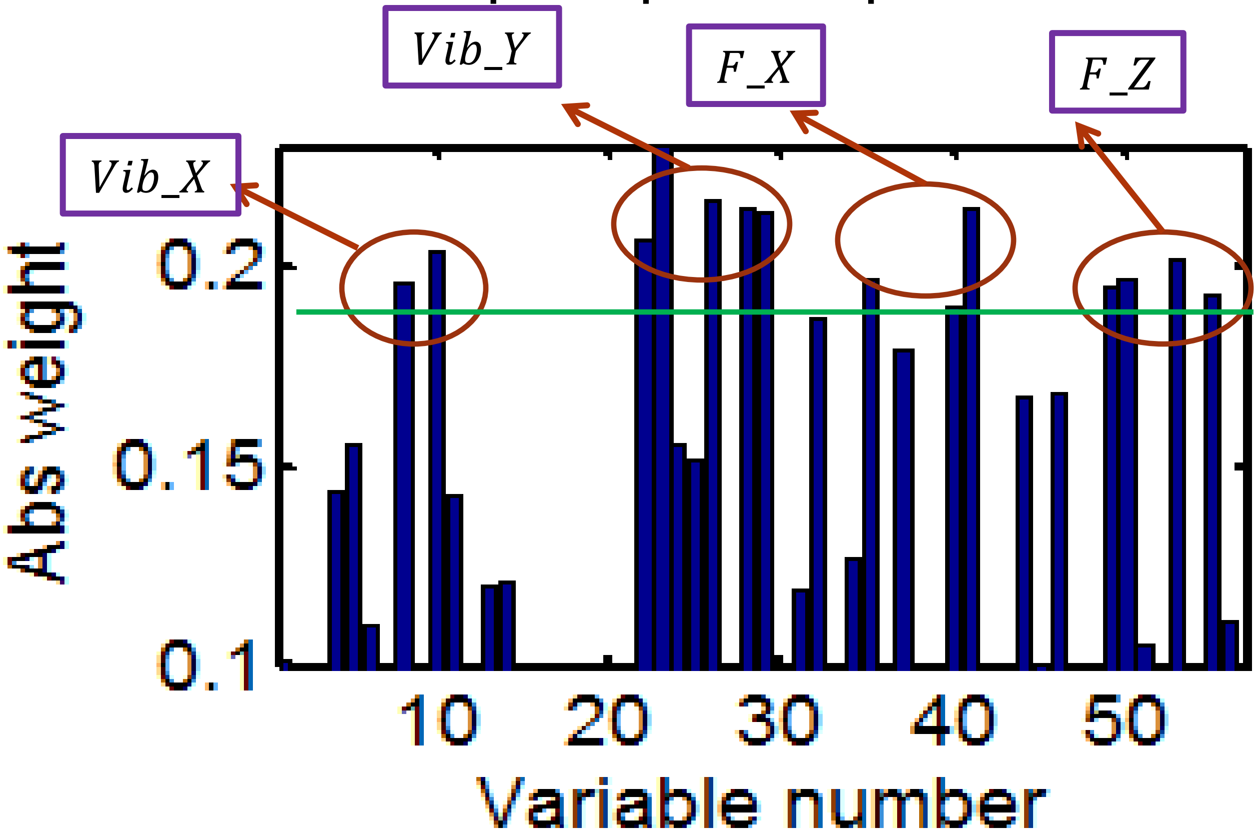

Gaussian process (GP) model

- Mapping between input $s \in R^{n_p}$ and $z \in R$

$$z = f(s) + \varepsilon \qquad \varepsilon \sim N(0, \sigma_1^2)$$

- Without explicit functional form, covariance structure can be used to represent the function value distribution

$$Z \sim N(0, K(S,S) + \sigma_1^2 I)$$

$$X = \left[s_1, s_2, \dots, s_{n_p}\right] \text{ and } Z = [z_1, z_2, \dots, z_{n_p}]$$

- Covariance matrix $K_{ij} = k_\theta(s_i, s_j)$, θ hyperparameters to be estimated
- Squared exponential form

$$k_\theta\left(s_i, s_j\right) = \sigma_0^2 \exp\left\{-\frac{(s_i - s_j)^T M (s_i - s_j)}{2}\right\} + \sigma_1^2$$

σ_0^2: process variance

σ_1^2: noise variance

$M = diag(l)^{-2}$: length scale in each input direction

- Infinitely differentiable; close points are highly correlated
- Log likelihood function to optimize the hyperparameters

GP prediction

- At new input $s_* \in R^{n_p}$, the noise-free prediction f_* is given by the first two moments

$$\bar{f}_* = K(S, s_*)^T (K(S,S) + \sigma_1^2 I)^{-1} Z$$

$$\mathrm{cov}(f_*) = K(s_*, s_*) - K(S, s_*)^T (K(S,S) + \sigma_1^2 I)^{-1} K(S, s_*)$$

- Can predict a complete distribution
  - $K(S, s_*)$: $n_p \times 1$ vector, each element is the covariance between s_* and one sample point
  - **Mean:** linear combination of the observation values
  - **Covariance:** difference between prior covariance and the information explained

Estimation result

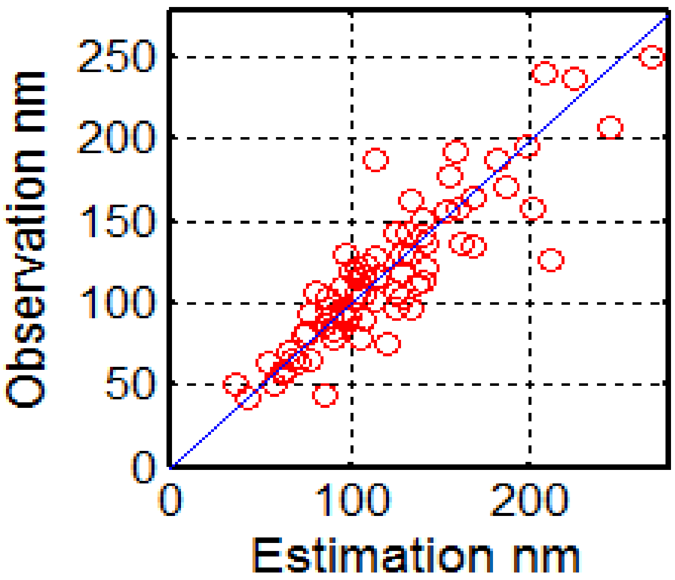

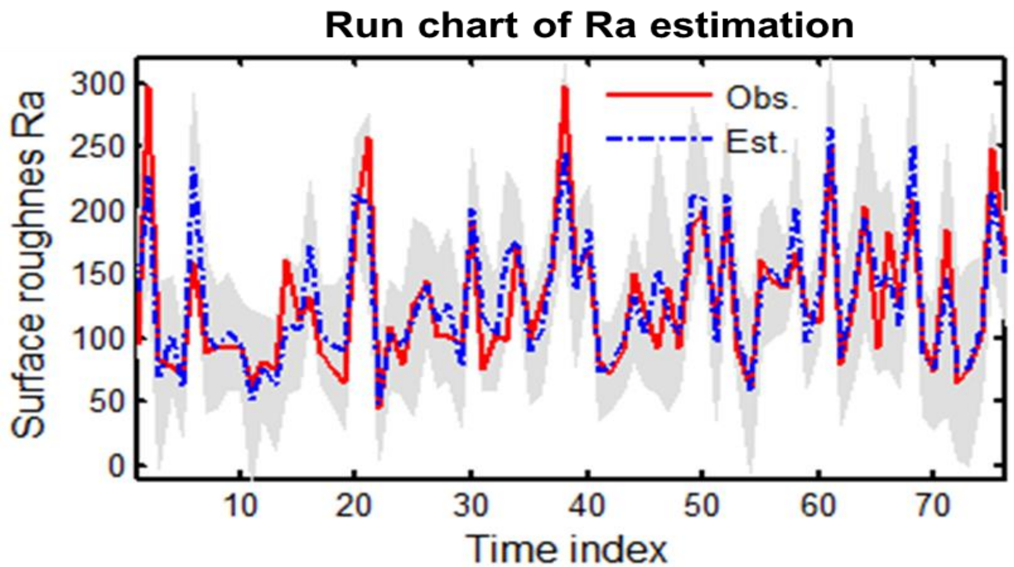

Over 85% of measured Ra values are within the 2-sigma prediction band

Accuracy of the fitting

	Mean	Standard deviation
R^2	0.83	0.11
RMS	21.4	4.37

Summary and future work

- **Summary**
  - **Physics-based model** can predict **chatter onset** according to process parameters; not applicable for real-time Ra estimation
  - **Physics-based statistical model** can estimate the surface roughness with accuracy over 80%
- **Future work**
  - Cutting **speed** and **thermal** effects on the thrust force
  - **Built-up edge effect:** dead metal cap on tool edge
  - **Uncertainty** in the stability analysis

Acknowledgement

- We acknowledge the generous support of the NSF (Grants CMMI 100978, 1301439).